Radiation force of coherent and partially coherent flat-topped beams on a Rayleigh particle

Chengliang Zhao,[1] Yangjian Cai,[1,2*] Xuanhui Lu,[1] and Halil T. Eyyuboğlu[3]

1. *Institute of Optics, Department of Physics, Zhejiang University, Hangzhou 310028, China*
2. *School of Physical Science and Technology, Suzhou University, Suzhou 215006, China*
3. *Department of Electronic and Communication Engineering, Çankaya University, Öğretmenler Cad. 14, Yüzüncüyıl 06530 Balgat Ankara, Turkey*

**Corresponding author: yangjian_cai@yahoo.com.cn*

Abstract: Propagations of coherent and partially coherent flat-topped beams through a focusing optical system are formulated. The radiation force on a Rayleigh dielectric sphere induced by focused coherent and partially coherent flat-topped beams is investigated theoretically. It is found that we can increase the transverse trapping range at the planes near the focal plane by increasing the flatness (i.e., beam order) of the flat-topped beam, and increase the transverse and longitudinal trapping ranges at the focal plane by decreasing the initial coherence of the flat-topped beam. Moreover the trapping stiffness of flat-topped beam becomes lower as the beam order increases or the initial coherence decreases. The trapping stability is also analyzed.

OCIS codes: (140.3295) Laser beam characterization; (140.7010) Laser trapping; (030.1640) Coherence; (030.1679) Coherence optical effect.

References and links

1. D. C. Cowan, J. Recolons, L. C. Andrews, and C. Y. Young, "Propagation of flattened Gaussian beams in the atmosphere: a comparison of theory with a computer simulation model," in *Atmospheric Propagation III,* C. Y. Young and G. C. Gilbreath, eds., Proc. SPIE **6215,** 62150B (2006).
2. H. T. Eyyuboğlu, A. Arpali, and Y. Baykal, "Flat topped beams and their characteristics in turbulent media," Opt. Express **14**, 4196-4207 (2006).
3. Y. Baykal and H. T. Eyyuboğlu, "Scintillation index of flat-topped Gaussian beams," Appl. Opt. **45**, 3793-3797 (2006).
4. Y. Cai, "Propagation of various flat-topped beams in a turbulent atmosphere," J. Opt. A: Pure Appl. Opt. **8**, 537-545(2006).
5. N. Nishi, T. Jitsuno, K. Tsubakimoto, S. Matsuoka, N. Miyanaga, and M. Nakatsuka, "Two-dimensional multi-lens array with circular aperture spherical lens for flat-top irradiation of inertial confinement fusion target," Opt. Rev. **7**, 216-220 (2000).
6. D. W. Coutts, "Double-pass copper vapor laser master-oscillator power-amplifier systems: Generation of flat-top focused beams for fiber coupling and percussion drilling," IEEE J. Quantum Electron. **38**, 1217-1224 (2002).
7. W. Wang, P. X. Wang, Y. K. Ho, Q. Kong, Z. Chen, Y. Gu, and S. J. Wang, "Field description and electron acceleration of focused flattened Gaussian laser beams," Europhys. Lett. **73,** 211-217 (2006).
8. L. Wang and J. Xue, "Efficiency comparison analysis of second harmonic generation on flattened Gaussian and Gaussian beams through a crystal CsLiB6O10," Jpn. J. Appl. Phys., Part 1, **41**, 7373-7376 (2002).
9. M. S. Bowers, "Diffractive analysis of unstable optical resonator with super-Gaussian mirrors," Opt. Lett. **19,** 1319-1321 (1992).
10. F. Gori, "Flattened gaussian beams," Opt. Commun. **107**, 335-341 (1994).
11. Y. Li, "Light beam with flat-topped profiles," Opt. Lett. **27**, 1007-1009 (2002).
12. A. A. Tovar, "Propagation of flat-topped multi-Gaussian laser beams," J. Opt. Soc. Am. A **18**, 1897-1904 (2001).
13. S. A. Amarande, "Beam propagation factor and the kurtosis parameter of flattened Gaussian beams," Opt. Commun. **129,** 311-317 (1996).
14. R. Borghi, M. Santarsiero, and S. Vicalvi, "Focal shift of focused flat-topped beams," Opt. Commun. **154,** 243-48 (1998).
15. V. Bagini, R. Borghi, F. Gori, A. M. Pacileo, and M. Santarsiero, "Propagation of axially symmetric flattened Gaussian beams," J. Opt. Soc. Am. A **13**, 1385-1394 (1996).

#104920 - $15.00 USD Received 4 Dec 2008; revised 19 Jan 2009; accepted 25 Jan 2009; published 29 Jan 2009

16. Y. Cai and Q. Lin, "Properties of a flattened Gaussian beam in the fractional Fourier transform plane," J. Opt. A: Pure Appl. Opt. **5**, 272-275 (2003).
17. X. Ji and B. Lu, "Focal shift and focal switch of flattened Gaussian beams in passage through an apertured bifocal lens," IEEE J. Quantum Electron. **39**, 172-178 (2003).
18. Y. Cai and Q. Lin, "Light beams with elliptical flat-topped profiles," J. Opt. A: Pure Appl. Opt. **6**, 390-395 (2004).
19. R. Borghi, "Elegant Laguerre-Gauss beams as a new tool for describing axisymmetric flattened Gaussian beams," J. Opt. Soc. Am. A. **18**, 1627-1633 (2001).
20. X. Lü and Y. Cai, "Analytical formulas for a circular or non-circular flat-topped beam propagating through an apertured paraxial optical system," Opt. Commun. **269**, 39-46 (2007).
21. G. Wu, H. Guo, and D. Deng, "Paraxial propagation of partially coherent flat-topped beam," Opt. Commun. **260**, 687-690 (2006).
22. Y. Cai and S. He, "Partially coherent flattened Gaussian beam and its paraxial propagation properties," J. Opt. Soc. Am. A **23**, 2623-2628 (2006).
23. R. Borghi and M. Santarsiero, "Modal decomposition of partially coherent flat-topped beams produced by multimode lasers," Opt. Lett. **23**, 313-315 (1998).
24. Y. Zhang, B. Zhang, and Q. Wen, "Changes in the spectrum of partially coherent flat-top light beam propagating in dispersive or gain media," Opt. Commun. **266**, 407-412 (2006).
25. M. Alavinejad and B. Ghafary, "Turbulence-induced degradation properties of partially coherent flat-topped beams," Opt. Lasers Eng. **46**, 357-362 (2008).
26. M. Alavinejad, B. Ghafary, and D. Razzaghi, "Spectral changes of partially coherent flat topped beam in turbulent atmosphere," Opt. Commun. **281**, 2173-2178 (2008).
27. Y. Baykal and H. T. Eyyuboğlu, "Scintillations of incoherent flat-topped Gaussian source field in turbulence," Appl. Opt. **46**, 5044-5050 (2007).
28. F. Wang and Y. Cai, "Experimental generation of a partially coherent flat-topped beam," Opt. Lett. **33**, 1795-1797 (2008).
29. A. Ashkin, "Acceleration and trapping of particles by radiation force," Phys. Rev. Lett. **24**, 156-159 (1970).
30. A. Ashkin, "Trapping of atoms by resonance radiation pressure," Phys. Rev. Lett. **40**, 729-732 (1978).
31. A. Ashkin, J. M. Dziezic, J. E. Bjorkholm, and S. Chu, "Observation of a single-beam gradient force optical trap for dielectric particles," Opt. Lett. **11**, 288-290 (1986).
32. Y. Harada and T. Asakura, "Radiation forces on a dielectric sphere in the Rayleigh scattering regime," Opt. Commun. **124**, 529-541 (1996).
33. P. Zemanek and C. J. Foot, "Atomic dipole trap formed by blue detuned strong Gaussian standing wave," Opt. Commun. **146**, 119-123 (1998).
34. M. Steven, S. B. Block Lawrence, and Goldstein & Bruce J. Schnapp, "Bead movement by single kinesin molecules studied with optical tweezers," Nature. **348**, 348 - 352 (1990).
35. L. Oroszi L, P. Galajda, H. Kirei, S. Bottka, and P. Ormos, "Direct measurement of torque in an optical trap and its application to double-strand DNA," Phys. Rev. Lett. **97**, 058301 (2006).
36. C. Day, "Optical trap resolves the stepwise transfer of genetic information from DNA to RNA," Phys. Today. **59**, 26-27 (2006).
37. S. Chu, J. E. Bjorkholm, A. Ashkin, and A. Cable, "Experimental observation and manipulation of stuck particles with pulsed optical tweezers," Opt. Lett. **30**, 1797-1799 (2005).
38. C. H. Chen, P. T. Tai, and W. F. Hsieh, "Bottle beam from a bare laser for single-beam trapping" Appl. Phys. Lett. **43**, 6001-6006 (2004).
39. J. Y. Ye. G. Q. Chang. T. B. Norris, C. Tse, M. J. Zohdy. K. W. Hollman, M. O'Donnell, and J. R. Baker, "Trapping cavitation bubbles with a self-focused laser beam," Opt. Lett. **29**, 2136- 2138 (2004).
40. M. Bhattacharya and P. Meystre, "Using a Laguerre-Gaussian Beam to Trap and Cool the Rotational Motion of a Mirror," Phys. Rev. Lett. **99**, 153603 (2007).
41. J. Tempere, J. T. Devreese, and E. R. I. Abraham, "Vortices in Bose-Einstein condensates confined in a multiply connected Laguerre-Gaussian optical trap," Phys. Rev. A **64**, 023603 (2001).
42. T. Meyrath, F. Schreck, J. Hanssen, C. Chuu, and M. Raizen, "A high frequency optical trap for atoms using Hermite-Gaussian beams," Opt. Express. **13**, 2843-2851 (2005).
43. K. Okamoto and S. Kawata, "Radiation Force Exerted on Subwavelength Particles near a Nanoaperture," Phys. Rev. Lett. **83**, 4534-4537 (1999).
44. Q. Zhan, "Trapping metallic Rayleigh particles with radial polarization," Opt. Express **12**, 3377-3382 (2004).
45. L. G. Wang, C. L. Zhao, L. Q. Wang, X. H. Lu, and S. Y. Zhu, "Effect of spatial coherence on radiation forces acting on a Rayleigh dielectric sphere," Opt. Lett. **32**, 1393-1395 (2007).
46. L. G. Wang and C. L. Zhao, "Dynamic radiation force of a pulsed Gaussian beam acting on a Rayleigh dielectric sphere," Opt. Express. **15**, 10615-10621 (2007).
47. Q. Lin, S. Wang, J. Alda, and E. Bernabeu, "Transformation of non-symmetric Gaussian beam into symmetric one by means of tensor ABCD law," Optik. **85**, 67-72 (1990).
48. J. A. Arnaud, "Nonorthogonal optical waveguides and resonators," Bell Syst. Tech. J. **49**, 2311-2348 (1970).

#104920 - $15.00 USD Received 4 Dec 2008; revised 19 Jan 2009; accepted 25 Jan 2009; published 29 Jan 2009

49. L. Mandel and E. Wolf, *Optical Coherence and Quantum Optics* (Cambridge, New York, 1995).
50. Q. Lin and Y. Cai, "Tensor *ABCD* law for partially coherent twisted anisotropic Gaussian Schell-model beams," Opt. Lett. **27**, 216-218 (2002).

1. Introduction

In recent years, light beams with flat-topped profiles have attracted more and more attention due to their wide applications in free-space optical communications, inertial confinement fusion, material thermal processing, nonlinear optics and electron acceleration [1-8]. Several theoretical models such as super Gaussian beam, flattened Gaussian beam, flat-topped beam and flat-topped multi-Gaussian beam have been proposed to describe a laser beam with flat-topped beam profile [9-12]. Propagations of various flat-topped beams in free-space, paraxial optical systems and turbulent atmosphere have been studied in detail [1,4, 9-20].

Recently, flat-topped beams have been extended to the partially coherent case. Several theoretical models have been proposed to describe a partially coherent beam with flat-topped beam profile [21, 22]. Borghi and Santarsiero studied the modal decomposition of partially coherent flat-topped beams [23]. Zhang et al. investigated the spectrum properties of a partially coherent flat-topped beam in dispersive and gain media [24]. M. Alavinejad studied the intensity and spectral properties of partially coherent flat-topped beams in turbulent atmosphere [25-26]. Baykal and Eyyuboğlu studied the scintillations of incoherent flat-topped Gaussian beam in turbulence [27]. More recently, Wang and Cai reported the experimental generation of a partially coherent flat-topped beam [28].

Light radiation force is produced by the exchange of momentum between photons and a micro-sized particle when the incident light is scattered by a particle as a whole. The use of radiation pressure for trapping and manipulation of particles is a subject of great interest. In 1970, Ashkin first demonstrated how to capture and manipulate micro-sized particles by using the radiation pressure [29]. Since then, this new technology has found wide applications in manipulating various particles such as micro-sized dielectric particles, neutral atoms, cells, DNA molecules, and living biological cells [30-37]. Up to now, the trapping characteristics of different beams, such as Gaussian beam, bottle beam, zero-order Bessel beam, Laguerre-Gaussian beam, Hermite-Gaussian beam, evanescent fields, radially polarized beam, Gaussian Schell-model beam and pulsed Gaussian beam have been studied [29-33, 38-46]. It has been found that the radiation forces produced by a laser beam are closely related to its beam characteristics such as beam profile, coherence and polarization. In this paper, we investigate the radiation force produced by focused coherent and partially coherent flat-topped beams on a Rayleigh particle. Some interesting and useful results are found.

2. The characteristics of coherent and partially coherent flat-topped beams

In this paper, we adopt the model for a flat-topped beam proposed by Li [11]. The electric field of a coherent flat-topped beam at z=0 can be expressed as a finite sum of fundamental Gaussian modes as follows [11],

$$E_{in-N}\left(\mathbf{r}, z=0\right) = E_{0N}\sum_{n=1}^{N}\frac{\left(-1\right)^{n-1}}{N}\binom{N}{n}\exp\left(-\frac{n\mathbf{r}^2}{w_0^2}\right), \tag{1}$$

where E_{0N} is a normalization factor, w_0 is the waist size of the fundamental Gaussian mode, $\binom{N}{n}$ denotes a binomial coefficient, and N is called the beam order of the flat-topped beam, When N=1, Eq. (1) reduces to the electric field of a Gaussian beam. Here we assume the power of the flat-topped beam to be P. Following [32], the power of a flat-topped beam is calculated by following formula

$$P = \int_{-\infty}^{+\infty}\int_{-\infty}^{+\infty} I_{in-N}(\mathbf{r}, z=0)dxdy, \tag{2}$$

#104920 - $15.00 USD Received 4 Dec 2008; revised 19 Jan 2009; accepted 25 Jan 2009; published 29 Jan 2009

where $I_{in-N}(\mathbf{r}, z=0) = \frac{n_m \varepsilon_0 c}{2} \left| E_{in-N}(\mathbf{r}, z=0) \right|^2$, n_m is the refractive index of the surrounding medium, ε_0 is the dielectric constant, and c is the speed of the light in vacuum. Substituting Eq. (1) into Eq. (2), we can obtain the expression for the normalization factor E_{0N} as follows

$$E_{0N} = \sqrt{4nP / \sum_{n=1}^{N} \frac{(-1)^{2(n-1)}}{N^2} \binom{N}{n} \pi w_0^2 n_m \varepsilon_0 c}. \tag{3}$$

The power of the flat-topped beam in this paper is set to be *P*=1W, which means every beam discussed in the following text carries the same power. Figure 1 shows the intensity distributions of a flat-topped beam for four different values of *N* with $w_0 = 10mm$. One finds from Fig. 1 that the beam profile becomes flatter (i.e., beam width increases) but the maximum intensity decreases as *N* increases, which means the potential wells of flatter beams (for example *N*=4, *N*=3) are *lower* or *shallower* than their counterparts (for example *N*=2, *N*=1). Fig. 1(b) is consistent with Fig. 1(a) of [11].

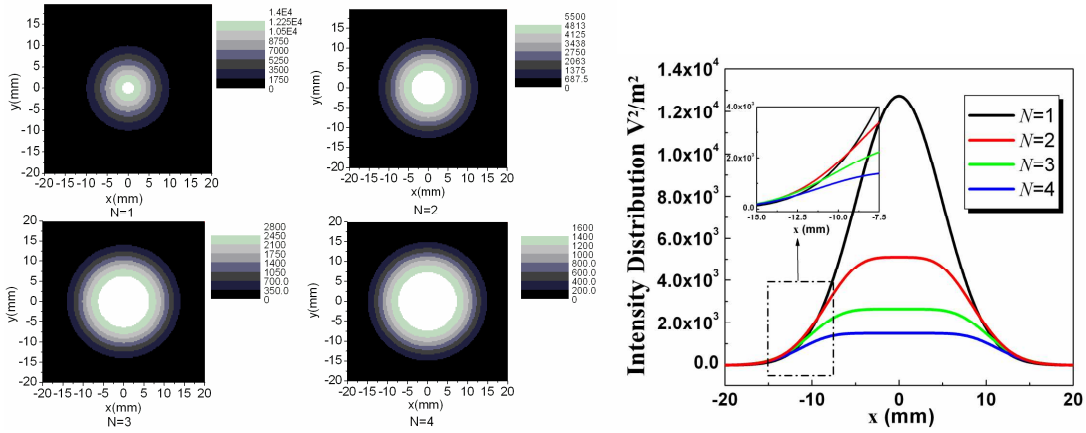

(a) (b)

Fig. 1. Intensity distribution of a flat-topped beam for four different values of *N* with $w_0 = 10mm$ (a) contour graph, (b) cross line (y=0)

After some arrangement, Eq. (1) can be expressed in following tensor form [18]

$$E_{in-N}(\mathbf{r}, z=0) = E_{0N} \sum_{n=1}^{N} \frac{(-1)^{n-1}}{N} \binom{N}{n} \exp\left(-\frac{ik}{2} \mathbf{r}^{\mathrm{T}} \mathbf{Q}_{1n}^{-1} \mathbf{r} \right), \tag{4}$$

where $\mathbf{r}^{\mathbf{T}} = (x \;\; y)$, $k = 2\pi / \lambda$ is the wave number with λ being the wavelength, $\mathbf{Q}_{1n}^{-1}$ is a 2×2 matrix named complex curvature tensor, and is given by

$$\mathbf{Q}_{1n}^{-1} = \begin{pmatrix} -2ni / kw_0^2 & 0 \\ 0 & -2ni / kw_0^2 \end{pmatrix}. \tag{5}$$

Within the validity of the paraxial approximation, by applying the tensor ABCD law [47, 48], we can express the electric field of a flat-topped beam in the output plane after passing through a general astigmatic (i.e., nonsymmetrical) optical system as follows [18]

$$E_{out-N}(\boldsymbol{\rho}, z) = E_{0N} \sum_{n=1}^{N} \frac{(-1)^{n-1}}{N} \binom{N}{n} \left[\det(\mathbf{A} + \mathbf{B}\mathbf{Q}_{1n}^{-1}) \right]^{-1/2} \exp\left(-\frac{ik}{2} \boldsymbol{\rho}^{T} \mathbf{Q}_{2n}^{-1} \boldsymbol{\rho} \right), \tag{6}$$

#104920 - $15.00 USD Received 4 Dec 2008; revised 19 Jan 2009; accepted 25 Jan 2009; published 29 Jan 2009

where det stands for the determinant, $\boldsymbol{\rho}$ is the position vector in the output plane given by $\boldsymbol{\rho}^{\mathrm{T}} = \left(\rho_x \quad \rho_y\right)$, $\mathbf{A}$, $\mathbf{B}$, $\mathbf{C}$ and $\mathbf{D}$ are the sub-matrices of the general astigmatic optical system, $\mathbf{Q}_{1n}^{-1}$ and $\mathbf{Q}_{2n}^{-1}$ are related by following tensor ABCD law

$$\mathbf{Q}_{2n}^{-1} = \left(\mathbf{C} + \mathbf{D}\mathbf{Q}_{1n}^{-1}\right)\left(\mathbf{A} + \mathbf{B}\mathbf{Q}_{1n}^{-1}\right)^{-1}. \tag{7}$$

The intensity of a coherent flat-topped beam at the output plane is given by $I_{out-N}\left(\boldsymbol{\rho}, z\right) = \frac{n_m \varepsilon_0 c}{2}\left|E_{out-N}\left(\boldsymbol{\rho}, z\right)\right|^2$.

For the more general case, we need to take the coherence of light into consideration. It is well known that a partially coherent beam can be characterized by the cross-spectral density. The cross-spectral density (z=0) of a partially coherent beam generated by a Schell-model source can be expressed in the following well-known form [49]

$$\Gamma\left(\mathbf{r}_1, \mathbf{r}_2, z=0\right) = \sqrt{I\left(\mathbf{r}_1, z=0\right) I\left(\mathbf{r}_2, z=0\right)}\, g\left(\mathbf{r}_1 - \mathbf{r}_2\right), \tag{8}$$

where $I\left(\mathbf{r}, z=0\right) = \Gamma\left(\mathbf{r}, \mathbf{r}, z=0\right)$ is the intensity distribution of the partially coherent beam, and $g\left(\mathbf{r}_1 - \mathbf{r}_2\right)$ is the spectral degree of coherence given by

$$g\left(\mathbf{r}_1 - \mathbf{r}_2\right) = \exp\left[-\frac{\left(\mathbf{r}_1 - \mathbf{r}_2\right)^2}{2\sigma_0^2}\right], \tag{9}$$

with σ_0 being the transverse spatial coherence width.

If the intensity distribution of a partially coherent flat-topped beam can be expressed as $I_{in-N}\left(\mathbf{r}, z=0\right) = \frac{n_m \varepsilon_0 c}{2}\left|E_{in-N}\left(\mathbf{r}, z=0\right)\right|^2$, we can express the cross-spectral density of a partially coherent flat-topped beam at z=0 as follows [21, 22]

$$\Gamma_{in-N}\left(\mathbf{r}_1, \mathbf{r}_2, z=0\right) = E_{0N}^2 \sum_{n=1}^{N}\sum_{m=1}^{N} \frac{(-1)^{n+m}}{N^2}\binom{N}{n}\binom{N}{m} \exp\left[-\frac{n\mathbf{r}_1^2 + m\mathbf{r}_2^2}{w_o^2} - \frac{\left(\mathbf{r}_1 - \mathbf{r}_2\right)^2}{2\sigma_0^2}\right], \tag{10}$$

In the incoherent limit (when $\sigma_0 = 0$), Eq. (10) reduces to

$$\Gamma_{in-N}\left(\mathbf{r}_1, \mathbf{r}_2, z=0\right) = E_{0N}^2 \sum_{n=1}^{N}\sum_{m=1}^{N} \frac{(-1)^{n+m}}{N^2}\binom{N}{n}\binom{N}{m} \exp\left(-\frac{n\mathbf{r}_1^2 + m\mathbf{r}_2^2}{w_o^2}\right)\delta\left(\mathbf{r}_1 - \mathbf{r}_2\right), \tag{11}$$

which denotes the cross-spectral density of an incoherent flat-topped beam. The two arbitrary transverse points of an incoherent flat-topped beam are correlated by δ function.

After some arrangement, Eq. (10) can be expressed in following tensor form

$$\Gamma_{in-N}(\tilde{\mathbf{r}}, 0) = E_{0N}^2 \sum_{n=1}^{N}\sum_{m=1}^{N} \frac{(-1)^{n+m}}{N^2}\binom{N}{n}\binom{N}{m} \exp\left(-\frac{ik}{2}\tilde{\mathbf{r}}^{\mathrm{T}}\mathbf{M}_{1nm}^{-1}\tilde{\mathbf{r}}\right), \tag{12}$$

where $\tilde{\mathbf{r}}^{\mathrm{T}} = (\mathbf{r}_1^{\mathrm{T}} \quad \mathbf{r}_2^{\mathrm{T}}) = (x_1 \quad y_1 \quad x_2 \quad y_2)$ and $\mathbf{M}_{1nm}^{-1}$ is a 4×4 complex matrix given by

$$\mathbf{M}_{1nm}^{-1} = \begin{bmatrix} \left(-\frac{2ni}{kw_0^2} - \frac{i}{k\sigma_0^2}\right)\mathbf{I} & \frac{i}{k\sigma_0^2}\mathbf{I} \\ \frac{i}{k\sigma_0^2}\mathbf{I} & \left(-\frac{2mi}{kw_0^2} - \frac{i}{k\sigma_0^2}\right)\mathbf{I} \end{bmatrix}, \tag{13}$$

#104920 - $15.00 USD Received 4 Dec 2008; revised 19 Jan 2009; accepted 25 Jan 2009; published 29 Jan 2009

here $\mathbf{I}$ is a 2×2 unit matrix. Within the validity of the paraxial approximation, by applying the tensor ABCD law of partially coherent beam [50], we can express the cross-spectral density of a partially coherent flat-topped beam after passing through a general paraxial astigmatic optical system as follows

$$\Gamma_{out-N}(\boldsymbol{\rho}_1,\boldsymbol{\rho}_2,z)=E_{0N}^2\sum_{n=1}^{N}\sum_{m=1}^{N}\frac{(-1)^{n+m}}{N^2}\binom{N}{n}\binom{N}{m}\left[\det\left(\overline{\mathbf{A}}+\overline{\mathbf{B}}\mathbf{M}_{1nm}^{-1}\right)\right]^{1/2}\exp\left(-\frac{ik}{2}\tilde{\boldsymbol{\rho}}^{\mathrm{T}}\mathbf{M}_{2nm}^{-1}\tilde{\boldsymbol{\rho}}\right), \tag{14}$$

where $\tilde{\boldsymbol{\rho}}^{\mathrm{T}}=(\boldsymbol{\rho}_1^{\mathrm{T}}\ \boldsymbol{\rho}_2^{\mathrm{T}})$, $\overline{\mathbf{A}}$, $\overline{\mathbf{B}}$, $\overline{\mathbf{C}}$ and $\overline{\mathbf{D}}$ are defined as follows:

$$\overline{\mathbf{A}}=\begin{pmatrix}\mathbf{A} & 0\mathbf{I}\\ 0\mathbf{I} & \mathbf{A}\end{pmatrix},\ \overline{\mathbf{B}}=\begin{pmatrix}\mathbf{B} & 0\mathbf{I}\\ 0\mathbf{I} & -\mathbf{B}\end{pmatrix},\ \overline{\mathbf{C}}=\begin{pmatrix}\mathbf{C} & 0\mathbf{I}\\ 0\mathbf{I} & -\mathbf{C}\end{pmatrix},\ \overline{\mathbf{D}}=\begin{pmatrix}\mathbf{D} & 0\mathbf{I}\\ 0\mathbf{I} & \mathbf{D}\end{pmatrix}. \tag{15}$$

$\mathbf{M}_{1nm}^{-1}$ and $\mathbf{M}_{2nm}^{-1}$ are related by following tensor ABCD law

$$\mathbf{M}_{2nm}^{-1}=(\overline{\mathbf{C}}+\overline{\mathbf{D}}\mathbf{M}_{1nm}^{-1})(\overline{\mathbf{A}}+\overline{\mathbf{B}}\mathbf{M}_{1nm}^{-1})^{-1}. \tag{16}$$

The intensity of a partially coherent flat-topped beam at the output plane is given by $I_{out-N}(\boldsymbol{\rho}_1,z)=n_m\varepsilon_0 c\Gamma_{out-N}(\boldsymbol{\rho}_1,\boldsymbol{\rho}_1,z)/2$. Although the intensity distribution of a partially coherent flat-topped beam at z=0 is independent of its initial coherence width (σ_0), the intensity distribution and the spatial coherence of flat-topped beam upon propagation are closely related to its initial coherence width (σ_0) as shown in Fig. 4 of next section and [22]. Partially coherent flat-topped beam has been generated in experiment recently [28]. Eqs. (6), (7) and (14)-(16) can be used to study the propagation properties of coherent and partially coherent flat-topped beams through paraxial optical systems conveniently.

3. The focusing properties of coherent and partially coherent flat-topped beams

In this section, we apply the formulae derived in section 2 to study the focusing properties of coherent and partially coherent flat-topped beams as shown in Fig. 2. In Fig. 2, a thin lens with focal length f is located at the input plane (z=0), and the output plane is located at $z=f+z_1$, where z_1 is the axial distance from the focal plane to the output plane. Then the transfer matrix between the input and output planes can be expressed as follows

$$\begin{pmatrix}\mathbf{A} & \mathbf{B}\\ \mathbf{C} & \mathbf{D}\end{pmatrix}=\begin{pmatrix}\mathbf{I} & (f+z_1)\mathbf{I}\\ \mathbf{0I} & \mathbf{I}\end{pmatrix}\begin{pmatrix}\mathbf{I} & 0\mathbf{I}\\ (-1/f)\mathbf{I} & \mathbf{I}\end{pmatrix}=\begin{pmatrix}(-z_1/f)\mathbf{I} & (f+z_1)\mathbf{I}\\ (-1/f)\mathbf{I} & \mathbf{I}\end{pmatrix}. \tag{17}$$

Substituting Eq. (17) into Eqs. (6) and (7), we calculate in Fig. 3 the intensity distribution of a focused coherent flat-topped beam for different values of *N* at several propagation distances with $f=10mm, w_0=10mm, \lambda=632.8nm$. One finds from Fig. 3 that the focusing properties of a flat-topped beam (*N*>1) are very interesting and different from that of Gaussian beam (*N*=1). At the focal plane ($z_1=0$), the intensity of the focused flat-topped beam is of quasi-Gaussian distribution, and maximum intensity decreases as the beam order *N* increases. When the output plane is a little away from the focal plane, the intensity of focused flat-topped beam becomes flat-topped, and the beam profile becomes flatter but the maximum intensity decreases as *N* increases. From Eq. (1), one can find that the flat-topped beam is not a pure mode, but a combination of different Gaussian modes, different Gaussian modes evolve differently upon propagation, what's more, different modes overlap and interfere during propagation, thus leading to the interesting focusing properties of flat-topped beam. More information about the propagation properties of the flat-topped beam can be found in [10]-[20].

#104920 - $15.00 USD Received 4 Dec 2008; revised 19 Jan 2009; accepted 25 Jan 2009; published 29 Jan 2009

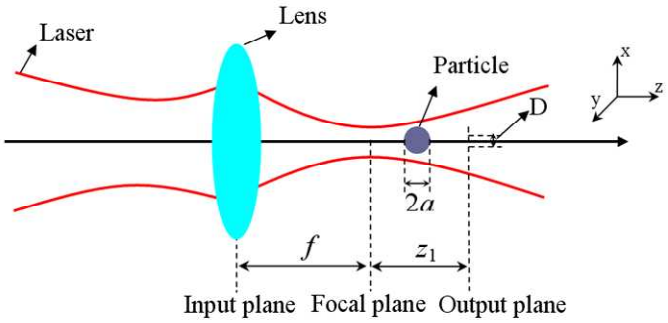

Fig. 2. Schematic of a focusing optical system

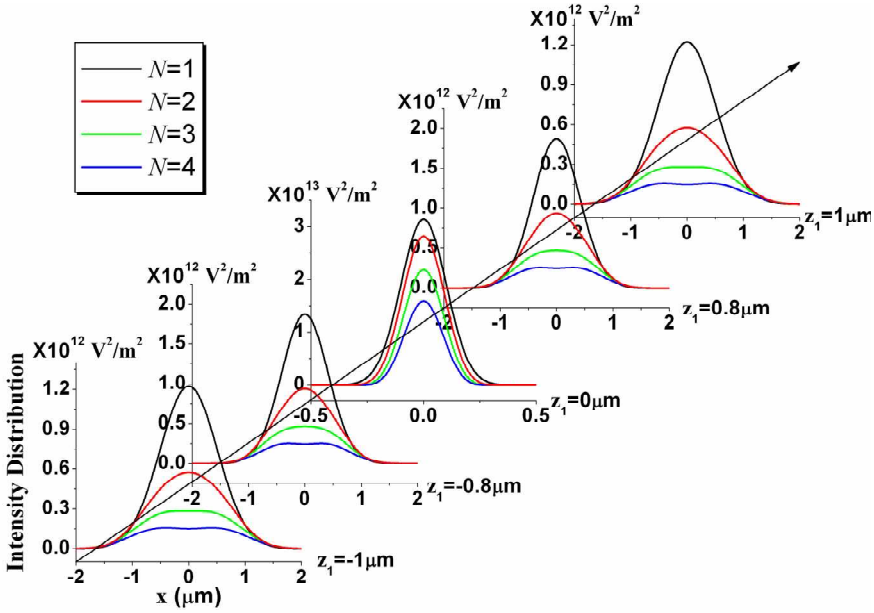

Fig. 3. Intensity distribution of a focused coherent flat-topped beam for different values of N at several propagation distances

Substituting Eq. (17) into Eqs. (14)-(16), we calculate in Fig. 4 the intensity distribution of a focused partially coherent flat-topped beam for different values of σ_0 (i.e., initial coherence) at several propagation distances. The other parameters take the same values with those used in Fig. 3. One finds from Fig. 4 that the intensity properties of a focused flat-topped beam are also closely related to its initial coherence. As the initial coherence decreases, the width of the focused beam spot at all propagation distances becomes large, which means a laser beam with high coherence can be focused more tightly as expected [49]. While the maximum intensity of the focused flat-topped beam decreases as the initial coherence decreases. What's more, the flat-topped beam profile at non-focal planes disappears gradually, and finally becomes a quasi-Gaussian beam profile as the initial coherence decreases.

#104920 - $15.00 USD Received 4 Dec 2008; revised 19 Jan 2009; accepted 25 Jan 2009; published 29 Jan 2009

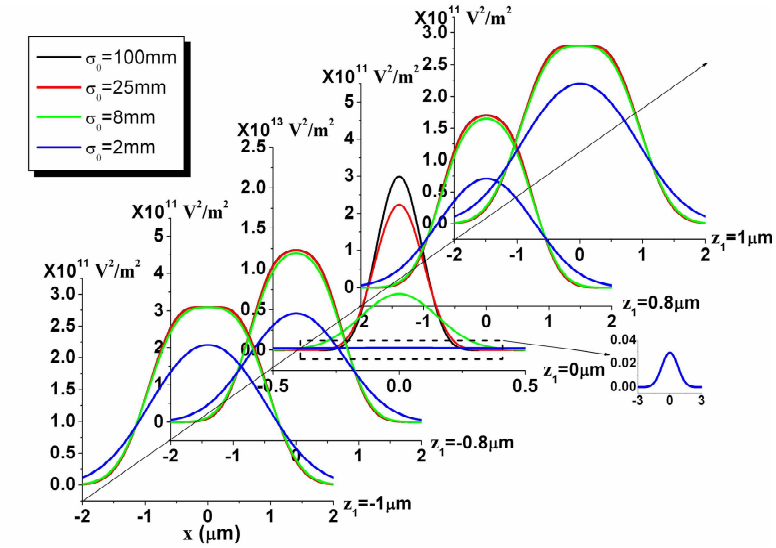

Fig. 4. Intensity distribution of a focused partially coherent flat-topped beam for different values of σ_0 at several propagation distances

4. Radiation force produced by focused coherent and partially coherent flat-topped beams on a Rayleigh particle

Now we study the radiation force produced by focused coherent and partially coherent flat-topped beams on a Rayleigh dielectric sphere, whose radius is much smaller than the wavelength of the laser beam (i.e., $a << \lambda$). The schematic for trapping a Rayleigh dielectric sphere with a focused flat-topped beam is shown in Fig. 2. A Rayleigh dielectric sphere with refractive index n_p is placed near the focus. In this case, the particle is treated as a point dipole. It's well known that there are two kinds of the radiation force: scattering force and gradient force. The scattering force F_{Scat} caused by the scattering of light by the sphere is proportional to light intensity and is along the direction of light propagation. The scattering force can be expressed as [32]

$$\vec{F}_{\text{Scat}}\left(\vec{\mathbf{r}},z\right)=\vec{e}_z n_m \alpha I_{out}/c, \tag{18}$$

where I_{out} is the intensity of the focused beam at the output plane, $\vec{e}_z$ is a unity vector along the beam propagation, $\alpha=\left(8/3\right)\pi(ka)^4 a^2[(\gamma^2-1)/(\gamma^2+2)]^2$, $\gamma=n_p/n_m$. The gradient force F_{Grad} produced by non-uniform electromagnetic fields is along the gradient of light intensity, and is expressed as [32]

$$\vec{F}_{Grad}\left(\vec{\mathbf{r}},z\right)=2\pi n_m \beta \nabla I_{out}/c, \tag{19}$$

where $\beta=a^3(\gamma^2-1)/(\gamma^2+2)$. By applying the Eqs. (6), (7), (14)-(16), (18) and (19), we can calculate the radiation force induced by focused coherent and partially coherent flat-topped beams on a Rayleigh dielectric sphere. We choose the radius of the particles to be $a=50$ nm, the refractive index of the particle to be $n_p=1.59$ (i.e., glass) and the refractive index of the ambient to be $n_m=1.33$ (i.e., water).

#104920 - $15.00 USD Received 4 Dec 2008; revised 19 Jan 2009; accepted 25 Jan 2009; published 29 Jan 2009

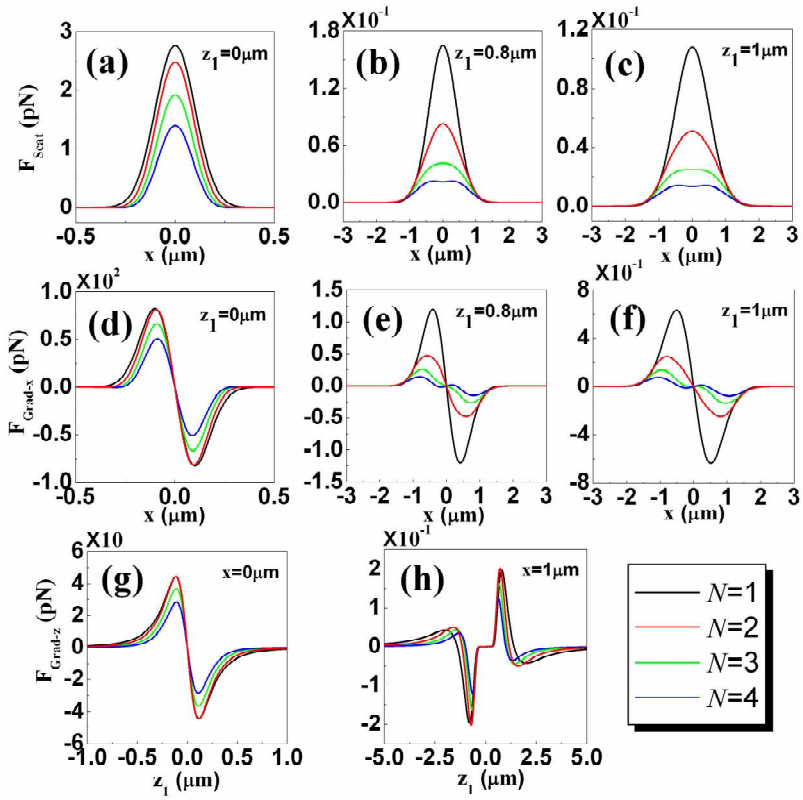

Fig. 5. The scattering force ((a)-(c)) and the transverse gradient force ((d)-(f)) of a coherent flat-topped beam for four different values of N at different positions z_1, and the longitudinal gradient force (g) and (f) for two different transverse positions x

We calculate in Figs. 5(a)-5(c) the scattering force (cross line y=0) and in Figs. 5(d)-5(f) the transverse gradient force (cross line y=0) of a coherent flat-topped beam for four different values of N at different positions z_1, and in Figs. 5(g) and 5(h) the longitudinal gradient force for two different transverse positions x. The sign of radiation force means the direction of the force. Positive F_{Scat} means the direction of the scattering force is along +z direction. Positive $F_{\text{Grad}-z}$ or $F_{\text{Grad}-x}$ means the direction of the gradient force is along +z or +x direction. One finds from Fig. 5 that both scattering force and gradient force decrease as the initial beam order N increases (i.e., beam profile becomes flatter), which means that the trapping stiffness (i.e., stability) of flatter beam is lower. What's more, the forward scattering force always is much smaller than the longitudinal gradient force, so the scattering force in this case can be neglected. From Figs. 5(d) and 5(g), one finds that at the focal plane ($z_1 = 0$), there is one stable equilibrium point, and we can use focused flat-topped beam to trap a Rayleigh particle whose refractive index is larger than the ambient at the focus. As the initial beam order N increases, the trapping stability decreases due to the decrease of radiation force, and both transverse trapping range and longitudinal trapping range becomes smaller (i.e., the positions of peak values approach the focus as N increases). So a coherent flat-topped beam (N>1) at the focal plane does not offer any advantage for trapping a Rayleigh particle over a Gaussian beam. From Figs. 5(e) and 5(f), one finds that we can increase the transverse trapping range (i.e., increase the width of potential well of flatter beam) by increasing the

#104920 - $15.00 USD Received 4 Dec 2008; revised 19 Jan 2009; accepted 25 Jan 2009; published 29 Jan 2009

initial beam order N suitably near the focal plane ($z_1 = 1\mu m$), even though the trapping stiffness decreases as N increases. Table 1 shows the trapping range of Fig. 5(f) for four different values of N. From Table 1 we can find that the trapping range increases remarkably as the beam order N increases. The trapping range for the case of N=4 is much large than the case of N=1 (Gaussian beam). But the initial beam order N can't be arbitrary large, because the trapping stability decreases with increasing N, as discussed in section 5. Rayleigh particles will diffuse instead of being trapped when N is very large (i.e., the trapping stiffness is very low) because the radiation forces are comparable to the Brownian force as shown later (see Fig. 8(a)). We also note from Fig. 5(h), because there are two stable equilibrium points, the particle can't be stably trapped along the z direction at off-axis points. To solve this problem, we can use two face to face focused flat-topped beams to construct a true optical potential well or "optical bottle" as shown in Fig. 6. To check for stability, we can interrupt one beam for a moment, which causes the particle to be accelerated rapidly in the remaining beam along its propagation direction. When another beam is turned on again, the particle is decelerated slowly and returns to its equilibrium region. So two face to face focused flat-topped beams can be used to trap a particle in a stable manner at on-axis and off-axis points.

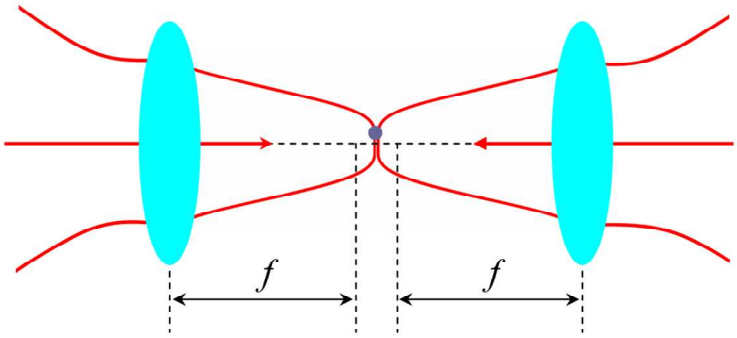

Fig. 6. Schematic of two face to face flat-topped beams focused on a particle

Table 1. The trapping range of Fig. 5(f) for four different values of N.

	Trapping Range D
N=1	10.2 a
N=2	16.0 a
N=3	19.0 a
N=4	21.1 a

Now we study the influence of coherence on radiation force produced by a partially coherent flat-topped beam. We calculate in Fig. 7(a)-7(c) the scattering force (cross line y=0) and in Fig. 7(d)-7(f) the transverse gradient force (cross line y=0) of a partially coherent flat-topped beam with N=3 for different values of σ_0 at different positions z_1, and in Fig. 7(g) and 7(h) the longitudinal gradient force for two different transverse positions x. One finds

#104920 - $15.00 USD Received 4 Dec 2008; revised 19 Jan 2009; accepted 25 Jan 2009; published 29 Jan 2009

from Fig. 7 that scattering force, transverse and longitudinal gradient forces decrease as the coherence of the initial flat-topped beam decreases. The forward scattering force also is much smaller than the longitudinal gradient force. From Figs. 7(d) and 7(g), we find that at the focal plane, as the initial coherence of flat-topped beam decreases, both transverse and longitudinal trapping ranges become larger (i.e., the positions of peak values deviate away from the focus as σ_0 decreases), while the trapping stiffness reduces due to the decrease of radiation force. Table 2 shows the trapping range of Fig. 7(d) for four different values of σ_0. The trapping range also increases remarkably as initial coherence width σ_0 decreases from Table 2. The trapping range for the case of $\sigma_0 = 2$ mm is much larger than the case of $\sigma_0 = 100$ mm. From Figs. 7(e), 7(f) and 7(h), we find at the planes near the focal plane, both trapping range and stability are reduced as the initial coherence of flat-topped beam decreases. Similarly, we can use two face to face focused partially coherent flat-topped beams to trap a particle in a stable manner at on-axis and off-axis points.

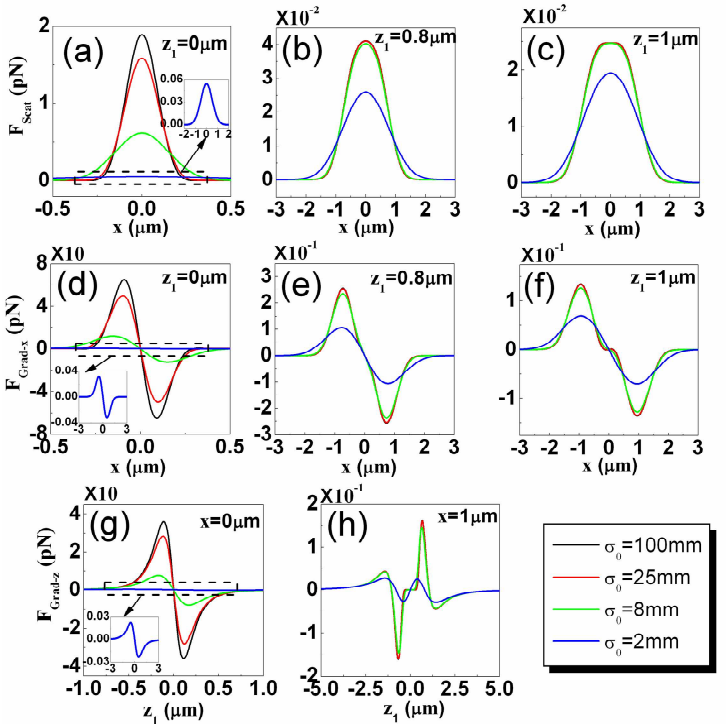

Fig. 7. The scattering force ((a)-(c)) and the transverse gradient force ((d)-(f)) of a partially coherent flat-topped beam with *N*=3 for different values of σ_0 at different positions z_1, and the longitudinal gradient force (g) and (f) for two different transverse positions x

#104920 - $15.00 USD Received 4 Dec 2008; revised 19 Jan 2009; accepted 25 Jan 2009; published 29 Jan 2009

Table 2. The trapping range of Fig. 7(d) for four different values of σ_0

	Trapping Range D
$\sigma_0 = 100$ mm	$1.8a$
$\sigma_0 = 25$ mm	$2.0a$
$\sigma_0 = 8$ mm	$3.0a$
$\sigma_0 = 2$ mm	$10.2a$

From above discussions, we can come to the conclusion that by increasing the flatness of the beam profile (i.e., increasing beam order *N*) of the flat-topped beam, we can increase the transverse trapping range at the planes near the focal plane. By decreasing the initial coherence of the flat-topped beam, we can increase the transverse and longitudinal trapping ranges at the focal plane. In both cases, the stability of trapping decreases, so it is necessary to choose suitable beam order *N* and initial coherence (i.e., σ_0) in order to extend the trapping range. This conclusion is the main result of present paper.

5. Analysis of the trapping stability

In this section, we analyze the trapping stability in detail by taking the Brownian motion into consideration. We know that the particle usually suffers from the Brownian motion due to the thermal fluctuation from the ambient (water). Following the fluctuation-dissipation theorem of Einstein, the magnitude of the Brownian force is expressed as $|F_B| = (12\pi\kappa a k_B T)^{1/2}$ [49], where κ is the viscosity of the ambient (in our case, $\kappa = 7.977 \times 10^{-4}$ Pas at the $T = 300$K), a is the radius of the particle and k_B is the Boltzmann constant. Then we obtain (after calculation) the magnitude of the Brownian force $F_B = 2.5 \times 10^{-3}$ pN. Comparing the radiation forces in Figs. 5 and Fig. 7, we can find that both scattering force and gradient force in our numerical examples are all larger than the Brownian force. So Brownian motion does not influence the main conclusion of present paper. We illustrate in Fig. 8 the dependencies of the radiation forces $F_{\text{Scat}}^{\text{Max}}$, $F_{\text{Grad-x}}^{\text{Max}}$ and $F_{\text{Grad-z}}^{\text{Max}}$ induced by a flat-topped beam on initial beam order *N* and initial coherence (i.e., σ_0) at z_1=0. For comparison, Brownian force F_B is also shown in Fig. 8. From Fig. 8(a), one finds that both scattering force and gradient force decrease as *N* increases, which is consistent with Fig. 5. When *N*=15, the scattering force equals Brownian force F_B, but the gradient force is still much larger than the scattering force and Brownian force F_B, so a flat-topped beam with *N*=15 can still be used to trap a particle. When *N*=20, the gradient force nearly equals the Brownian force F_B, so a flat-topped beam with $N \geq 20$ cannot be used for trapping a particle. From Fig. 8(b), one finds that both scattering force and gradient force decrease as the initial coherence of flat-topped beam decreases, which is consistent with Fig. 8. When σ_0 is smaller than 0.04, we cannot use a partially coherent flat-topped beam for trapping a particle because the Brownian force is larger than the radiation force. The line Q in Figs. 8 (a) and 8(b) can be regarded as the critical line. From above discussions, we come to conclusion that the trapping stability decreases as the initial beam

#104920 - $15.00 USD Received 4 Dec 2008; revised 19 Jan 2009; accepted 25 Jan 2009; published 29 Jan 2009

order increases or initial coherence decreases, and we should choose suitable values of N and σ_0 of flat-topped beam for particle trapping.

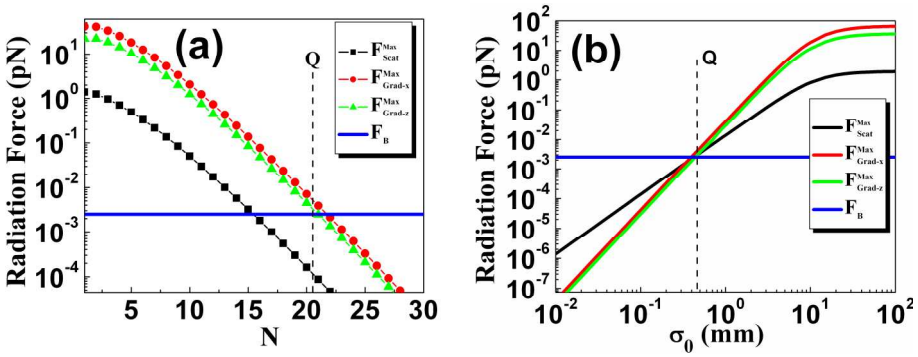

Fig. 8. (a) Dependence of the radiation forces $F_{\text{Scat}}^{\text{Max}}$, $F_{\text{Grad-x}}^{\text{Max}}$ and $F_{\text{Grad-z}}^{\text{Max}}$ produced by a coherent flat-topped beam on initial beam order N at z_1=0, (b) Dependence of the radiation forces $F_{\text{Scat}}^{\text{Max}}$, $F_{\text{Grad-x}}^{\text{Max}}$ and $F_{\text{Grad-z}}^{\text{Max}}$ produced by a focused partially coherent flat-topped beam on σ_0 at z_1=0 with N=3. F_{B} is the Brownian force

6. Conclusion

In conclusion, we have studied the focusing properties of coherent and partially coherent beams, and have studied the radiation force on a Rayleigh dielectric sphere induced by focused coherent and partially coherent flat-topped beams. We have found that we can increase the transverse trapping range at the planes near the focal plane by increasing the flatness (i.e., beam order) of flat-topped beam, and we can increase the transverse and longitudinal trapping ranges at the focal plane by decreasing the initial coherence of the flat-topped beam. We have also found that the trapping stability decreases as the flatness of flat-topped beam increases or as the initial coherence decreases. So it is necessary to choose suitable beam order and initial coherence of a flat-topped beam in order to trap a particle. Our results are interesting and useful for particle trapping.

Acknowledgments

This research is supported by the Hi-Tech Research and Development Program of China (863 Project, Grant No. 2007AA12Z130). Y. Cai gratefully acknowledges support from the Alexander von Humboldt Foundation.

#104920 - $15.00 USD Received 4 Dec 2008; revised 19 Jan 2009; accepted 25 Jan 2009; published 29 Jan 2009